JOURNAL OF NEUROTRAUMA 33: 2202–2216 (December 15, 2016)

DOI: 10.1089/neu.2016.4439

The Evaluation of Magnesium Chloride within a Polyethylene Glycol Formulation in a Porcine Model of Acute Spinal Cord Injury

Femke Streijger,[1] Jae H.T. Lee,[1] Neda Manouchehri,[1] Elena B. Okon,[1] Seth Tigchelaar,[1] Lisa M. Anderson,[1] Greg A. Dekaban,[2] David A. Rudko,[3] Ravi S. Menon,[4] Jennifer F. Iaci,[5] Donald C. Button,[5] Andrea M. Vecchione,[5] Andrey Konovalov,[5] Patrick D. Sarmiere,[5] Chi Ung,[5] Anthony O. Caggiano,[5] and Brian K. Kwon[1,6]

Abstract

A porcine model of spinal cord injury (SCI) was used to evaluate the neuroprotective effects of magnesium chloride ($MgCl_2$) within a polyethylene glycol (PEG) formulation, called ''AC105'' (Acorda Therapeutics Inc., Ardsley, NY). Specifically, we tested the hypothesis that AC105 would lead to greater tissue sparing at the injury site and improved behavioral outcome when delivered in a clinically realistic time window post-injury. Four hours after contusion/compression injury, Yucatan minipigs were randomized to receive a 30-min intravenous infusion of AC105, magnesium sulfate ($MgSO_4$), or saline. Animals received 4 additional infusions of the same dose at 6-h intervals. Behavioral recovery was tested for 12 weeks using two-dimensional (2D) kinematics during weight-supported treadmill walking and the Porcine Injury Behavior Scale (PTIBS), a 10-point locomotion scale. Spinal cords were evaluated *ex vivo* by diffusion-weighted magnetic resonance imaging (MRI) and subjected to histological analysis. Treatment with AC105 or $MgSO_4$ did not result in improvements in locomotor recovery on the PTIBS or in 2D kinematics on weight-supported treadmill walking. Diffusion weighted imaging (DWI) showed severe loss of tissue integrity at the impact site, with decreased fractional anisotropy and increased mean diffusivity; this was not improved with AC105 or $MgSO_4$ treatment. Histological analysis revealed no significant increase in gray or white matter sparing with AC105 or $MgSO_4$ treatment. Finally, AC105 did not result in higher Mg^{2+} levels in CSF than with the use of standard $MgSO_4$. In summary, when testing AC105 in a porcine model of SCI, we were unable to reproduce the promising therapeutic benefits observed previously in less-severe rodent models of SCI.

Key words: AC105; magnesium; polyethylene glycol; porcine; spinal cord injury

Introduction

It has been recognized for many years that injury to the central nervous system (CNS) results in a significant reduction of magnesium ions (Mg^{2+}) within the brain and spinal cord,[1,2] and that the decreases in systemic, cerebrospinal fluid (CSF), and intracellular Mg^{2+} concentrations are closely associated with severity of neurological impairment.[1–6] After CNS injury, excitotoxic glutamate release can cause overstimulation of post-synaptic glutamate receptors, including N-methyl-D-aspartate (NMDA) receptors. The opening of these receptors allows for further influx of sodium and calcium, producing a calcium overload, which may cause further cell injury and death.[7] The widespread distribution of NMDA receptors throughout the CNS has prompted extensive study of NMDA-receptor antagonists as potential neuroprotective agents. Because magnesium physiologically provides a voltage-dependent blockade of calcium entry through the NMDA receptor,[8] magnesium is one such agent whose neuroprotective properties have been well established in the laboratory setting.

[1]International Collaboration on Repair Discoveries (ICORD), University of British Columbia, Blusson Spinal Cord Center, Vancouver, British Columbia, Canada.
[2]Robarts Research Institute, Western University, London, Ontario, Canada.
[3]Brain Imaging Center, Montreal Neurological Hospital and Institute, Montreal, Quebec, Canada.
[4]Center for Functional and Metabolic Mapping, the University of Western Ontario, London, Ontario, Canada.
[5]Acorda Therapeutics Inc., Ardsley, New York.
[6]Department of Orthopedics, Vancouver Spine Surgery Institute, University of British Columbia, Blusson Spinal Cord Center, Vancouver, British Columbia, Canada.

Systemically administered magnesium sulfate ($MgSO_4$) has been extensively investigated in rodent models of acute SCI and has been reported by numerous independent investigators to improve outcome.[9–13] Though this demonstrates a fairly robust ''proof of principle,'' significant histological and functional benefits were only demonstrated following extremely high doses of magnesium (300–600 mg/kg), which far exceeds the 2- to 6-g bolus dose of intravenous (i.v.) magnesium sulfate ($MgSO_4$) currently recommended for the treatment of pre-eclampsia or cardiac arrest.[14,15] Notably, in a randomized, controlled trial, toxicity was observed when extremely large doses of $MgSO_4$ were given for neuroprotection after traumatic brain injury (TBI).[16] This mismatch between the high concentrations of systemic Mg^{2+} needed to produce beneficial CNS effects in animal models, the relatively low systemic concentrations that are found to be clinically tolerable, and the relative impermeability of the CNS to magnesium delivered through the vasculature[17] underlay further initiatives to determine whether combining Mg^{2+} with polyethylene glycol (PEG) would reduce the Mg^{2+} dosage needed to induce effective neuroprotection.

AC105 is a proprietary magnesium chloride ($MgCl_2$) formulation in PEG, a hydrophilic polymer used as an excipient for many pharmacological agents (Acorda Therapeutics Inc., Ardsley, NY). It was developed as a therapeutic intervention for acute spinal cord injury (SCI) and was subsequently reported to be neuroprotective in compressive and contusive models of thoracic and cervical SCI in the rat.[11,18,19] Treating animals with AC105 decreased lesion volumes by 67%, and open field locomotion (Basso, Beattie, Bresnahan) scores were significantly improved compared to a saline-treated group (10.0 ± 0.2 vs. 7.8 ± 0.4).[19] Importantly, the doses of magnesium in the AC105 formulation (5 infusions of 190 μmol/kg) used in the rodent thoracic and cervical SCI model by Kwon and colleagues[19] and Lee and colleagues,[18] respectively, were within the range of human tolerability and comparable to doses that previously have appeared to be safe in clinical trials of stroke and cardiac arrest (4 g of bolus within 12 h post-injury, followed by 16 g over 24 h).[20–25] A comparison between $MgSO_4$-PEG and $MgCl_2$-PEG showed no statistical difference between the two salts, but the investigators noted that the AC105-treated group appeared to have slightly better locomotor recovery early post-SCI.[19]

The aim of the present study was to test AC105 within a large animal model of SCI, using a recently described porcine model.[26] Both AC105 and an equivalent dose of magnesium within a clinically available $MgSO_4$ formulation without PEG were evaluated in this experiment. Nonclinical optimization studies, in addition to toxicity, safety pharmacology and pharmacokinetic studies, and previous published experience with i.v. magnesium in large-scale clinical trials were all considered in deriving a dosage regimen for AC105 of 5 i.v. infusions of 0.2 mmol of Mg^{2+}/kg/infusion, with each dose being delivered over 30 min by a pump-controlled infusion at 6-h intervals for a total dose of 1.0 mmol of Mg^{2+}/kg/24 h. Using this dosage regime, we evaluated the effect of AC105 on behavioral recovery over 12 weeks (using two-dimensional [2D] kinematic analysis and the Porcine Thoracic Injury Behavioral Score [PTIBS]) and on tissue sparing around the injury site (using ultra-high resolution anatomical and diffusion-weighted magnetic resonance imaging [MRI] as well as histologic analysis). Longitudinal blood samples were also evaluated for glial fibrillary acidic protein (GFAP) levels as a potential biomarker of treatment response. Longitudinal sampling of

Table 1. Animals and Grouping

Group	*Injury model*	*Intervention*	*Body weight (kg) [average ± SEM]*	*Impact force (kdyn) [Average ± SEM]*
SHAM ($n=4$)	Laminectomy surgery only	n.a.	23.5 22.0 21.0 20.5 [21.8 ± 0.66]	n.a.
SCI+saline ($n=6$)	T10 weight drop 50 g; 20 cm height; 5′ 150 g compression	• Saline (5 mL/kg) • i.v. infusion over 30 min • Initiated 4 h post-SCI • Then every 6 h for a total of 5 doses	24.0 23.0 23.5 22.0 21.0 21.5 [22.3 ± 0.49]	2632 2713 1665 3266 3150 3589 [2836 ± 276]
SCI+$MgSO_4$ ($n=6$)	T10 weight drop 50 g; 20 cm height; 5′ 150 g compression	• $MgSO_4$ (47.4 mg/kg $MgSO_4$ heptahydrate diluted in 0.9 % sodium chloride (5 mL/kg) • i.v. infusion over 30 min • Initiated 4 h post-SCI • Then every 6 h for a total of 5 doses	21.0 21.5 21.5 21.0 21.5 21.5 [21.3 ± 0.11]	3611 2995 3147 3517 3658 3227 [3359 ± 111]
SCI+AC105 ($n=6$)	T10 weight drop 50 g; 20 cm height; 5′ 150 g compression	• AC105 (5 mL/kg yielding 39.1 mg/mL of $MgCl_2$ heptahydrate) • i.v. infusion over 30 min • Initiated 4 h post-SCI • Then every 6 h for a total of 5 doses	23.0 20.5 23.0 22.0 22.5 25.0 [22.6 ± 0.67]	3236 2856 1764 3559 3260 3329 [3000 ± 264]

SCI, spinal cord injury; $MgSO_4$, magnesium sulfate; n.a., not applicable; i.v., intravenous; $MgCl_2$, magnesium chloride; SEM standard error of the mean.

cerebrospinal fluid (CSF) was also done to analyze the biodistribution of magnesium within the injured CNS.

Methods

All animal training and procedures were performed in accord with the guidelines of the Canadian Council for Animal Care and approved by our institution's animal care committee. All analyses were performed by personnel blinded to the three treatment groups.

Animals and treatment details

Female Yucatan miniature pigs (Sinclair Bio-Resources, Columbia, MO) were group housed at our large animal facility for at least 5 week before surgery. At surgery, animals' mean weight was 22.19 ± 0.28 kg. Three groups of $n = 6$ pigs each were subjected to experimental SCI (Table 1). At 4 h post-SCI, animals were randomized to receive either 1) saline (5 mL/kg), 2) AC105 (5 mL/kg yielding 39.1 mg/kg of $MgCl_2$ heptahydrate) over a 30-min period, or 3) $MgSO_4$ (47.4 mg/kg of $MgSO_4$ heptahydrate diluted in 0.9% sodium chloride [5 mL/kg; provided by Vancouver General Hospital) over a 30-min period by i.v. infusion, which was repeated every 6 h for a total of 5 doses. Dosages of AC105 used in this study were similar to those evaluated in previous rodent SCI studies.[18,19] In addition to the three experimental treatment groups, a fourth group of ''sham'' animals ($n = 4$), which received exactly the same surgical procedure as the SCI group but sustained no contusion injury or treatment, was included to serve as a baseline ''uninjured'' condition for the MRI and histological analysis (Table 1).

Surgical procedures

After the animal was anesthetized, the external jugular vein was catheterized for blood sampling. Using a scalpel, a longitudinal incision was made on the ventral aspect of the neck ~ 3 cm left of the midline. The left jugular vein was exposed by blunt dissection using hemostats and an 8F Groshong catheter was inserted ~ 10 cm toward the heart (product no. 7707540, M.R.I. implantable ports; Bard Canada Inc., Oakville, Ontario, Canada). The catheter was tunneled subcutaneously (s.c.) to an area near the neck where a collection port (product no. 7707540, M.R.I. implantable ports; Bard Canada Inc.) buried just beneath the skin was attached. After venous catheterization, the animal was positioned prone for SCI surgery as described in Lee and colleagues.[26] Briefly, a midline incision was made in the thoracic region to expose the underlying muscle. Using electrocautery, the incision was carried through the fascia and down to the spinous processes. A laminectomy was performed from T9 to T14 to expose the thecal sac and underlying spinal cord. The laminectomy was widened at T10 to ensure that the impactor tip did not contact the bony edges of the laminectomy during the course of the impact. T14 was also widened to allow the intrathecal insertion of a catheter for CSF collection (B. Braun Medical Inc., Bethlehem, PA). The catheter was brought through the s.c. tissue and attached to a collection port (product no. MIDLOA, LOVOL MIN ports; Instech Laboratories, Plymouth Meeting, PA) that was positioned on the back of the animal for repeated CSF sampling. Pedicle screws were inserted bilaterally into T9, T10, and T11 (3.5-mm Vertex Screws; Medtronic, Minneapolis, MN), and the guide rail for the weight drop impactor system was secured rigidly to these screws, immobilizing the spine over these three segments. At T10, a 50-g weight was dropped down the guide-rail from a height of 20 cm and an additional 100 g was carefully added for 5 min to provide sustained extradural compression. The weight drop apparatus was removed and titanium rods were secured to the pedicle screws bilaterally to achieve rigid fixation along the T9–T11 segments. After the injury, the muscles and skin were closed with multiple layers of sutures. The animal was removed from the ventilator and intubation and allowed to regain consciousness.

Cerebrospinal fluid and blood sampling

The first blood and CSF samples were drawn 20 min pre-SCI (sample 1). The thoracic SCI was then induced, denoted as ''Time 0.'' Blood and CSF samples were drawn at 30 min, 1 h, and 2 h post-injury (samples 2, 3, and 4). Another sampling was done at 4 h post-injury (sample 5), infusion of saline, AC105, or $MgSO_4$ began for 30 min. A ''mid-infusion'' sample of blood and CSF was drawn 15 min after the infusions began (sample 6). Samples were taken at the indicated time points (Table 2). At each sampling time point, 200 μL of CSF and 5 mL of blood were collected. CSF samples were centrifuged at 1000 rcf for 10 min, aliquoted, and snap frozen. Blood samples were allowed to sit at room temperature for 30 min to allow for clotting; samples were then centrifuged at 10,000 rcf for 5 min. Serum was aspirated off, aliquoted, and snap frozen.

Table 2. CSF and Blood Sampling Schedule

Sample	*Time post-SCI*	*Comments*
1	−1 h	
	0 h	Thoracic SCI
2	0.5	First sample post-injury
3	1	
4	2	
5	4	Immediately before the initiation of infusion no. 1
6	4	AC105 infusion no. 1 over 0.5 h CSF/serum sample taken 15 min after infusion starts
7	5	0.5 h post-infusion no. 1
8	6	1.5 h post-infusion no. 1
9	10	Immediately before the initiation of infusion no. 2
	10	AC105 infusion no. 2 over 0.5 h
10	11	0.5 h post-infusion no. 2
11	12	1.5 h post-infusion no. 2
12	16	Immediately before the initiation of infusion no. 3
	16	AC105 infusion no. 3 over 0.5 h
13	17	0.5 h post-infusion no. 3
14	18	1.5 h post-infusion no. 3
15	22	Immediately before the initiation of infusion no. 4
	22	AC105 infusion no. 4 over 0.5 h
16	23	0.5 h post-infusion no. 4
17	24	1.5 h post-infusion no. 4
18	28	Immediately before the initiation of infusion no. 5
19	28	AC105 infusion no. 5 over 0.5 h CSF/serum sample taken 15 min after infusion starts
20	29	0.5 h post-infusion no. 5
21	30	1.5 h post-infusion no. 5
22	48	2 days post-injury
23	72	3 days post-injury
24	96	4 days post-injury
25	120	5 days post-injury
26	144	6 days post-injury
27	168	7 days post-injury
28	@ Euthanasia	3 months post-injury

CSF, cerebrospinal fluid; SCI, spinal cord injury.

These samples were then sent to Acorda Therapeutics: the CSF for analysis of Mg^{2+} concentrations to assess the biodistribution of magnesium, and the serum for analysis of GFAP as a potential biomarker of injury severity and treatment response.

The Porcine Thoracic Injury Behavior Scale

Pigs were delivered 5 weeks before the scheduled surgery. After acclimatization and habituation to the large animal facility (1 week), animals were handled within their pens daily for 4 days to become familiar with experimental handling. Then, animals underwent 1 h of training each day for 5 days to walk upon command up and down a rubber mat (width, 1.22 m; length, 5 m) without stopping.[26] Before injury, animals were videotaped to establish the ''baseline'' locomotor behavior. This was captured on three high-definition camcorders positioned behind the animals to visualize the movements of the hindlimbs and rump as they walked away from the cameras. Videotaping of locomotor recovery resumed 1 week post-injury and continued weekly for 12 weeks in total. The natural progression in hindlimb function was analyzed and classified into 10 different stages using the Porcine Thoracic Injury Behavioral Scale (PTIBS),[26] ranging from no active hindlimb movements (score, 1) to normal ambulation (score, 10). PTIBS scores of 1–3 are characterized by ''hindlimb dragging,'' scores of 4–6 reflect varying degrees of ''stepping'' ability, and scores of 7–10 reflect varying degrees of ''walking'' ability.

Two-dimensional hindlimb kinematics during weight-supported treadmill locomotion

For 2D kinematic analysis of hindlimb function, animals were trained to walk on the treadmill each day for a minimum of 3 weeks before surgery. Animals were first trained in pairs using allotted daily food portions until fully accustomed to the treadmill setup. Further training was done individually to build endurance on the treadmill to 6 min of walking without interruption at 1.5 mph. After initial treadmill training, animals were then acclimated to wear a harness around their trunk, which was attached to a pulley supported by a metal frame surrounding the treadmill; this pulley system could then be adjusted to support between 0% and 100% of the animals' body weight. During training and pre-injury assessments, no weight support was provided while the animals walked on the treadmill. After SCI surgery, animals were 100% weight supported. Reflective markers were positioned on each animal's four hindlimb joints, including the fetlock joints, hock joint, stifle joint, and hip joint; a marker was also placed on the pelvis as a relatively stationary control. The same operator performed all marker placements to minimize variability in the marker position. The reflective markers were illuminated by a light source placed 75 cm away from the treadmill. After the animals fully acclimated to the treadmill setup, stepping capacities were recorded preoperatively (week 0), 2 weeks postoperatively, and then weekly until the end of the experiment (week 12).

Kinematic data were collected for 6 min at a treadmill speed of 1.5 mph, which is within the normal walking velocity. Two high-definition cameras were placed perpendicular to the direction of the movement to obtain a lateral view of the hindlimbs. Kinematic data were collected at a sampling rate of 60 frames per second. After collection, joint positions were digitized using semiautomatic tracking (Dartfish Software). Joint angle trajectories for the left hindlimb were then calculated from joint positions. To account for variations in gait cycle time, each gait cycle was time normalized to 60 data points using MATLAB software (The MathWorks, Inc., Natick, MA). Zero gait cycle was defined as onset of stance phase, which was determined from video recordings and defined as the time when the hoof was in its anterior extreme position (AEP). Gait cycle was defined as the time from one AEP event to the next. Similarly, swing phase onset was defined as the time when the toe was in its posterior extreme position. Once normalized, joint angular trajectories were averaged across each step to compute average trajectories for each animal. Mean trajectories of the hip, stifle, tarsal, and metatarsals were evaluated by averaging the first 4–10 consecutive steps, depending upon how many steps the animal took. Stifle and hock joint angles were defined as included angles between the shank and thigh segments and shank and foot segments, respectively. The hip angle was defined as the angle between the thigh and the pelvis segment. In all cases, increasing angle values indicate extension. Vertical values of extension were defined as the maximum value of angular position during the stance phase of the gait cycle. Peak values of flexion-flexor moment were defined as the minimum value. Peak values from each step cycle were determined and averaged per animal.

The vector between the metatarsal and hip marker positions was computed from the digitized points with custom MATLAB software (The MathWorks Inc.). The vertical direction describes movement in the dorsoventral plane relative to the hip marker position referred to vertical displacement (limb length). The linear anterior-posterior (horizontal direction) orientation of the hindlimb to the hip marker is referred to as horizontal displacement (step length). A value of ''0'' indicated the position of the hip marker, negative values indicated that the corresponding joint marker remained behind (horizontal displacement) or below (vertical displacement) the position of the hip marker. These kinematic analyses were performed using custom-written programs in MATLAB.

Ex vivo *magnetic resonance imaging of spinal cord*

Twelve weeks post-injury, animals were euthanized and a spinal cord segment of 10 cm with the lesion epicenter located centrally was immediately fixed in 4% paraformaldehyde (PFA) for 12 h and then stored in 0.1% PFA. These spinal cord sections were sent to Robarts Research Institute at the University of Western Ontario (London, Ontario, Canada) for conventional and diffusion tensor imaging (DTI) MRI scanning. All imaging was performed on an Agilent 9.4 Tesla, small animal MRI scanner (Agilent Technologies, Santa Clara, CA). An in-house designed B_0 (main magnetic field) mapping sequence, RASTAMAP,[27] was employed to perform automated higher-order B_0 field shimming before all imaging. This alleviates image distortion and reduces imaging errors attributed to off-resonance effects. After shimming, high-resolution (100-mm isotropic resolution) anatomical images were acquired to provide a reference with which to compare DTI and histology data. Anatomical images were acquired using a three-dimensional balanced steady-state free precession (bSSFP) MRI sequence.

Scan parameters for the bSSFP sequence were as follows: coronal plane image orientation; TR (repetition time) = 13.1 ms; TE (echo time) = 6.6 ms; excitation pulse flip angle = 30 degrees; bandwidth = 50 kHz; field of view (FOV) = $51.2 \times 12.8 \times 12.8$ mm^3; resolution = $0.1 \times 0.1 \times 0.1$ mm^3; and eight offline signal averages. Total scan duration for this sequence was 2 h and 13 min.

DTI was performed using a 2D, axial orientation, diffusion-weighted spin-echo sequence with TR = 2000 ms, TE = 23.91 ms, excitation pulse flip angle = 90 degrees, acquisition bandwidth = 25 kHz, FOV = 12.8×12.8 mm^2, in-plane resolution = 0.1×0.1 mm^2, slice thickness = 0.75 mm, 65 slices, 12 diffusion encoding directions, and two signal averages. A b-value of 1000 s/mm^2 was used for diffusion weighting. Total scan duration was 1 h and 51 min. DTI data were processed offline using the FSL tool, DTIFIT,[28–32] to generate maps of primary eigenvector, eigenvalue, mean diffusivity, and fractional anisotropy. The resulting indices of fractional anisotropy (FA) and mean diffusivity (MD) were compared with histology from the same spinal cords.

Eriochrome cyanine R staining

After MRI imaging, spinal cord segments were cryoprotected using a graded concentrations of sucrose (6, 12, and 24% sucrose in

0.1 M of phosphate buffer each for 48 h). Tissue was then embedded in Tissue-TekTM CRYO-OCT compound (Sakura Finetek, Torrance, CA) and frozen before being cut into serial 20-μm-thick transverse sections using a cryostat. Every other section was mounted on a series of 10× silane-coated slides, such that the adjacent sections mounted on each slide represented regions spaced 400 μm apart. For differentiating gray and white matter, Eriochrome cyanine R staining was performed on spinal cord sections, which specifically stains myelin sheaths blue. This staining procedure is outlined by Rabchevsky and colleagues.[33] Briefly, sections were dehydrated in an ethanol series, cleared in xylene, rehydrated in a reverse ethanol series followed by distilled water (dH_2O), then left in a solution containing 0.16% Eriochrome cyanine R, 0.5% sulphuric acid, and 0.4% iron chloride (in dH_2O) to stain myelinated fibres. After staining, sections were differentiated in 0.5% ammonium hydroxide. After differentiation, gray matter was counterstained in Neutral Red, then rinsed in dH_2O. Finally, sections were dehydrated and cleared, as described above, and then mounted onto silane-coated SuperFrost-Plus slides (Fisher Scientific, Pittsburgh, PA).

Quantification of tissue sparing

Distribution of spared white and gray matter was mapped using digital color images of Eriochrome cyanine (EC)-stained sections as well as scanned MRI images:

1. EC-stained sections were examined using a Zeiss AxioImager M2 microscope (Carl Zeiss, Jena, Germany), and pictures were taken of sections at 800-μm intervals throughout the lesion site. Images were analyzed using Zen Imaging Software, which allowed the tracing of the spinal cord perimeter and spared tissue for each image captured, giving the total area for each of these measurements. Lesion area was identified by loss of EC staining as well as severe tissue disruption.

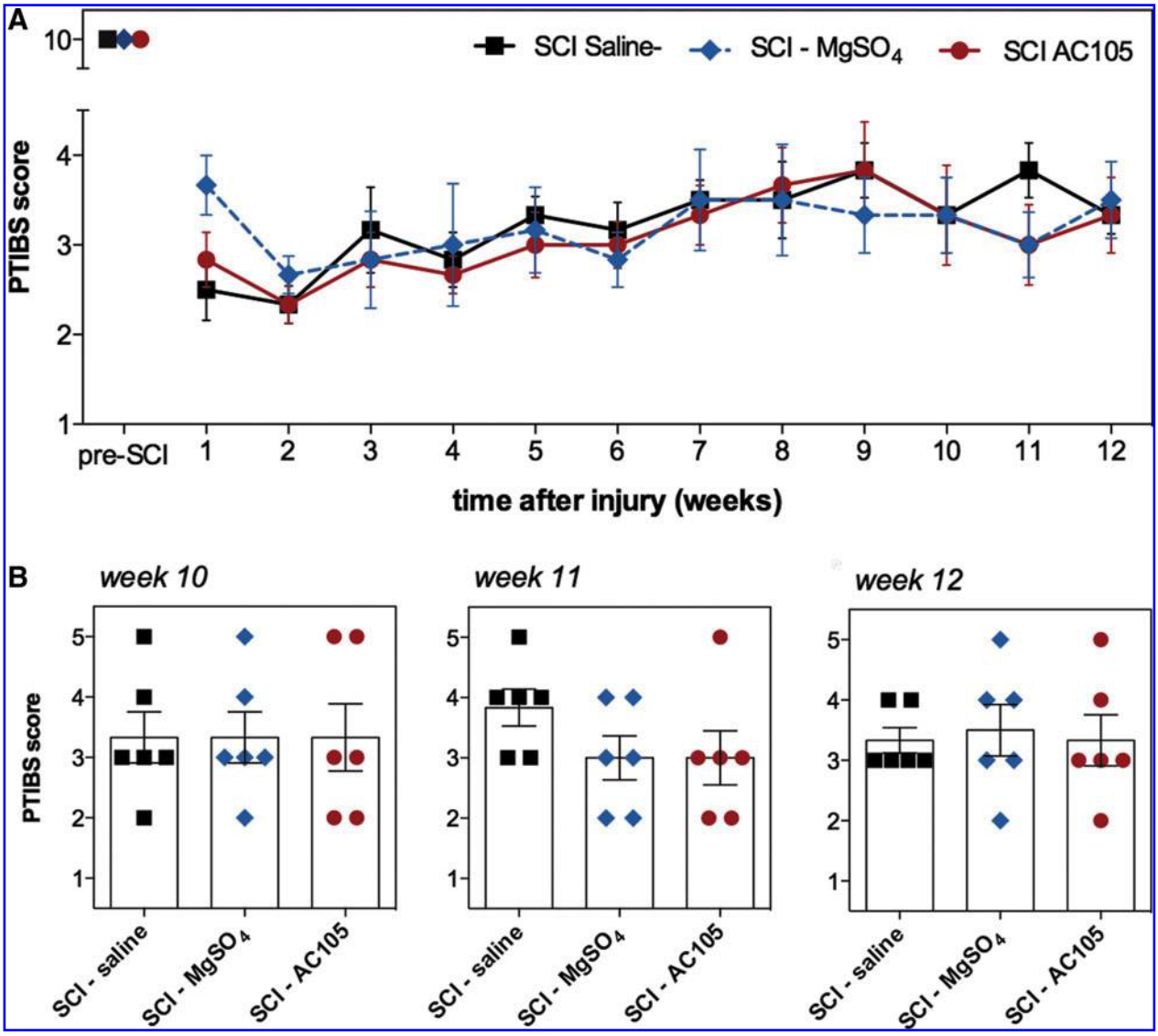

FIG 1. Behavioral recovery during overground locomotion. (**A**) Locomotor function was determined by PTIBS (Porcine Thoracic Injury Behavior Scale) testing in pigs treated with either saline ($n=6$), $MgSO_4$ ($n=6$), or AC105 ($n=6$). Values are means ± standard error of the mean (SEM). (**B**) Scatter plots of individual values for PTIBS score for weeks 10–12. Each bar represents the mean ± SEM. No significant differences in PTIBS score are found pre-operatively (baseline) or at any post-operative time points between the three groups. $MgSO_4$, magnesium sulphate; SCI, spinal cord injury. Color image is available online at www.liebertpub.com/neu

The lesion epicenter was defined as the section from each animal with the least amount of white matter sparing, and quantification was carried out at 800-μm intervals from 14.4 mm caudal to 14.4 mm rostral to the epicenter. Spared white matter was defined as the areas that were stained for EC, whereas gray matter was considered spared when it was a stereotypic light grey color with a consistent neuropil texture containing neuronal and glial cell bodies.

2. Spared tissue areas from T2-weighted images were outlined manually using ImageJ software (National Institutes of Health, Bethesda, MD). Myelin has relatively short T2 and T1 relaxation times, primarily attributed to its lipid content. As a result, normal myelin is hypointense to gray matter on T2-weighted images. If a disease process reduces the myelin content, the white matter becomes less hydrophobic and takes on more water. Less myelin and more water protons prolong the relaxation times of T2, resulting in more signal on T2-weighted images.

For both assessments, extent of spared white matter and gray matter were calculated as the percentage of total area of the spinal cord (i.e., area within the tracing of spinal cord perimeter), with lesion epicenter located centrally. The same person blinded to the initial treatment allocation and subsequent behavioral results manually traced both type of images.

Measurement of serum glial fibrillary acidic protein

Serum samples were received on dry ice and maintained at approximately −80°C at Acorda Therapeutics, Inc. until analyzed. Serum samples were analyzed for levels of GFAP by electrochemiluminescence immunosandwich assay on the MesoScale Discovery (MSD) platform. Briefly, samples were diluted 1:1 with a TBS/BSA buffer and combined with an antibody master mix containing both biotin-labeled mouse anti-GFAP (no. 556327; BD Biosciences, San Jose, CA) and sulfo-tagged rabbit anti-GFAP (#Z0334; Dako, Carpinteria, CA). The sample/antibody mixture was incubated to come to equilibrium for 2 h with mild shaking. At the same time, a Streptavidin Gold Detection Plate was blocked with MSD Blocker A. After incubation, 50 μL of the equilibrated sample/antibody mixture was added to the pre-blocked detection plate, which was then incubated for 1 h to allow the antibody/GFAP complex to bind the surface of the streptavidin plate. The plate was washed to remove all unbound material, 150 μL of MSD Read Buffer was added to each well, and plates were read immediately after addition of the read buffer. Each plate was run with a calibration curve and quality control standards handled as the samples. The detection range of the assay was determined to be 0.098–72.000 ng/mL in neat serum.

Measurement of cerebrospinal fluid magnesium

Samples of CSF were analyzed for levels of Mg^{2+} by optical emission spectroscopy with inductively-coupled plasma excitation (OES-ICP) using a Spectro Analytical Instruments Genesis EOP II (Spectro Analytical Instruments, Kleve, Germany). Briefly, samples stored at –80°C were thawed at room temperature, mixed well, and then triplicate 25-μL aliquots were each diluted with 4.975 g of distilled H_2O to achieve a 200-fold dilution of analyte in a 5-mL sample volume. Samples were introduced to OES-ICP by an automated sample injection system through a cross-flow nebulizer at pump setting 2. Mg^{2+} signal was acquired from the 279.553 emission line using the following instrument configuration: 1400 W of plasma power; coolant flow, 12 L/min; and nebulizer flow, 0.83 L/min. Carryover of analyte between analyzed samples was effectively eliminated by extensive rinsing with water between each sample injected. To monitor consistency of instrument response over the several hours required to perform each samples analysis run, a series of calibration reference standard samples containing Mg^{2+} ranging from 0 to 2000 parts per billion were also analyzed at the beginning of each batch run and after every 12 analyzed CSF samples.

Results

Porcine Thoracic Injury Behavior Scale

PTIBS scoring was performed pre-operatively and then on a weekly basis post-injury to assess changes in gross locomotor performance (Fig. 1). Before SCI surgery, all animals achieved a baseline score of 10, indicative of normal hindlimb function and locomotion. Post-SCI, locomotor function was most severely impaired acutely post-injury, with a mean PTIBS score of 2–3 at 1 week post-injury (Fig. 1). This represents extensive hindlimb movements with or without weight bearing extension, which lifts the rump and knees transiently off the floor. Minimal spontaneous recovery was observed over the next 6-week period post-injury, with a mean PTIBS score of 3–4 by 7 weeks post-injury, indicating that animals were capable of weight bearing extensions either transiently or constantly (i.e., score 3 or 4). For the majority of the animals, there was still a complete lack of stepping (the presence of at least two steps with the rump and knee constantly off the ground during the steps would be assigned a score of 5). Spontaneous recovery plateaued at this point, with PTIBS scores remaining between 3 and 4 by the final week of the study (12 weeks post-injury).

At all post-injury time points (from weeks 1 to 12), all animals were substantially and significantly impaired compared to baseline values, independent of their treatment. No significant differences in PTIBS scores between treatment groups were found at any time point tested. Animals in the SCI-saline group had a mean PTIBS score of 3.33 ± 0.21 at the 12-week time point, whereas SCI animals treated with $MgSO_4$ and AC105 had a mean PTIBS score of 3.50 ± 0.43 and 3.33 ± 0.42, respectively (Fig. 1).

Two-dimensional kinematic analysis

Post-injury, the number of step cycles accomplished was limited by the poor weight-bearing capability of the animals.

FIG. 2. Hindlimb kinematics during fully weight-supported treadmill locomotion. (**A**) Duration of stance, (**B**) swing phase, and (**C**) swing/stance duration expressed as a percentage of the total gait cycle duration at 10–12 weeks post-injury. Each bar represents the mean ± standard error of the mean. Dots represent individual animals. Post-SCI, the absolute swing duration became interrupted, with longer durations compared to pre-injury. Stance duration was less affected. No statistical differences between groups were observed. (**D**) Step cycle trajectories. Forward and backward movements are indicated by the filled and open symbols, respectively. The trajectories shown are group averages. Only the trajectories from pigs that performed at least 4 steps were included in this analysis ($n = 3$ of 6 SCI; $n = 9$ of 9 intact). Data from the contused pigs are from tests performed 10–12 weeks post-contusion. (**E**) Mean maximum vertical and horizontal displacement relative to the hip marker (value "0") of the stifle, hock, and fetlock. A negative value indicates that the hindlimb is positioned behind or remains below the hip marker; positive values that the hindlimb is in front of the position of the hip marker. For the AC105 group, an abrupt vertical trajectory of the fetlock with minimal horizontal displacement is observed, resulting in step heights values similar to intact pre-injury values. *$p < 0.05$. $MgSO_4$, magnesium sulphate; SCI, spinal cord injury. Color image is available online at www.liebertpub.com/neu

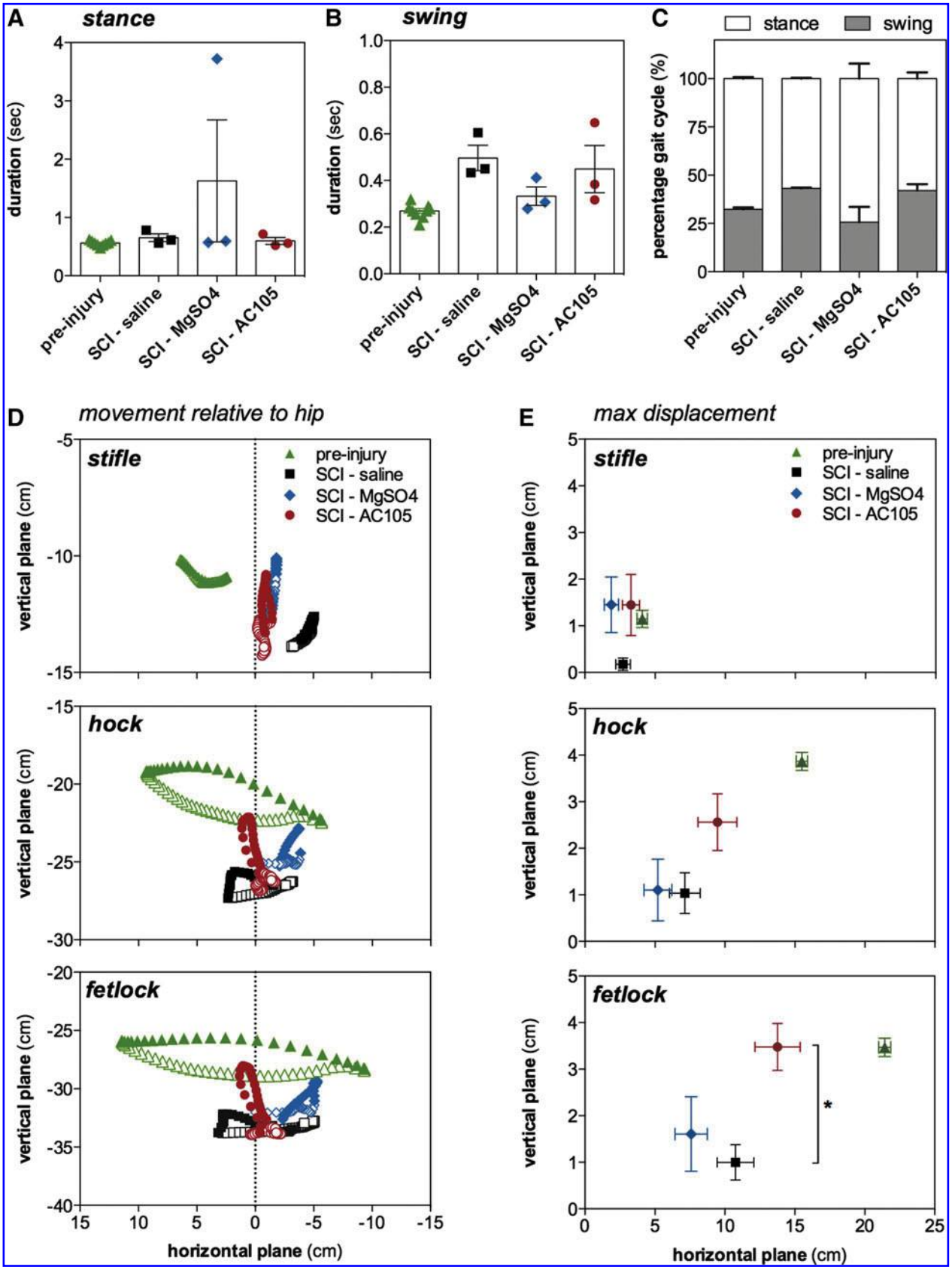

Although fully weight supported, animals did not demonstrate hindlimb stepping on the treadmill until they acquired a PTIBS score of 4 or higher (capable of active rhythmic hindlimb crawling with constant or transient hindquarter elevation). Therefore, the results of the 2D kinematic analysis represent only 3 of the 6 animals from each group that achieved a PTIBS score of 4. Animals with a PTIBS score of 3 or lower typically dragged their legs on the treadmill.

Post-injury, relative and absolute swing duration became disrupted, with longer duration of the swing phase compared to pre-injury levels from 0.269 ± 0.010 to 0.497 ± 0.055 sec ($p = 0.012$; Fig. 2A–C). Duration of the stance phase was much less affected, with a mean value of 0.653 ± 0.066 sec post-injury compared to 0.562 ± 0.015 sec pre-injury. Second, maximum vertical displacement of the hock and fetlock markers decreased to approximately 25% of pre-injury values, whereas horizontal displacement decreased to 50% (Fig. 2D,E).

SCI animals treated with $MgSO_4$ and AC105 showed a similar ability to perform stepping on the treadmill compared to the saline-treated group. Peak values of joint angular position of the hip, stifle, and hock joints did not differ between treatment groups (saline, $MgSO_4$, and AC105) during forward or backward movement while stepping on a treadmill (Fig. 2). In addition, stance time, swing time, and horizontal displacement did not differ between treatment groups (Fig. 2). However, the AC105 group did move their fetlock with a different trajectory shape relative to the saline-treated group (Fig. 2D). At the onset of the swing phase, an abrupt vertical trajectory of the metatarsal occurred during forward movement in the AC105 group, resulting in a maximal vertical displacement of 3.48 ± 0.44 cm compared to 0.99 ± 0.25 ($p = 0.008$) and 1.61 ± 1.11 cm ($p = 0.19$) for respectively the saline and $MgSO_4$ group (Fig. 2E).

Ex vivo *magnetic resonance imaging assessment of white and gray matter microstructural integrity*

Spinal cord gray matter of uninjured control animals was hyperintense compared with white matter (Supplementary Fig. 1) (see online supplementary material at http://www.liebertpub.com). In injured animals, at the lesion center, spinal cord diameter was reduced and the gray/white matter differentiation completely lost. The homogenous hyperintense signal intensity was pronounced in the spinal cord center and diminished toward the surface of the cord. Round/oval well-demarcated areas of hyperintense signal were found on the axial images both rostral and caudal to the lesion epicenter, consistent with cystic cavitation. These were well visualized as elliptical cavities on the sagittal MRI images, potentially representing early syrinx formation.

Two frequently applied quantitative diffusion parameters can be derived from DTI data: 1) MD, quantifying the overall magnitude of water diffusion, and 2) FA, reflecting the directionality of water diffusion and coherence of white matter fiber tracts. These measures are related to the microstructural organization of white matter and are used to infer structural characteristics of the local tissue environment. Representative images of FA and MD in axial slices of spinal cord are shown in Figures 3 and 4. At all points in the white matter, MD values significantly increased post-surgery compared with the value pre-surgery (Fig. 3C,D). Similarly, MD values of the gray matter post-surgery increased significantly (to a value of approximately 1.6×10^{-3} mm^2/s) throughout the volume of the spinal cord (30 mm) when compared with those pre-surgery (0.5×10^{-3} mm^2/s; Fig. 3A,B).

For FA, values equal to 0 correspond to isotropic diffusion (equal water diffusion in all directions). By contrast, higher FA values (closer to 1) are observed in cases where restricted diffusion of water occurs along a single plane. Such is the case, for example, with water diffusion in myelinated fiber tracts in brain tissue. Pre-SCI, the pig white matter had elevated FA (0.60–0.70) values relative to the more isotropic value (0.3–0.4) obtained in gray matter (Fig. 4A,B). Post-injury, the FA of both white and gray matter was consistently lower (suggestive of loss of axonal integrity) with minimal values between 0.2 and 0.3 at the lesion epicenter (Fig. 4C,D). No significant group differences were found for either FA or MD in gray or white matter.

Histological assessment of spared gray and white matter

In order to quantify the extent of spared tissue at the lesion epicenter as well as the rostrocaudal spread of the injury, quantification of spared gray and white matter was performed on serial sections stained with Eriochrome cyanine R (Fig. 5). At week 12 post-SCI, there was severe destruction at the lesion epicenter, where significant destruction of both gray and white matter was present. We defined the core of the lesion as all areas that were not significantly different from the epicenter. The boundaries of this lesion core were the shortest distance rostral and caudal from the epicenter, where the areas were significantly different from the area at the epicenter. At 12 weeks post-SCI, the length of this core at T10 was approximately 6.4 mm in the saline-treated SCI group. The core of the lesion extended 8.0 and 9.6 mm, respectively, in AC105- and $MgSO_4$-treated pigs. Quantification of the spared white and gray matter area showed no differences between saline- and $MgSO_4$-treated animals (Fig. 6). In both the saline and $MgSO_4$ groups, the total cross-sectional area was greater in the most rostral and caudal areas up to ~ 7.2 mm to the epicenter compared to the sham group, indicative of diffuse edema. Although such cord swelling was less evident for the AC105 group, no significant difference was observed between treatment groups (Fig. 6). Both white and gray matter at the lesion epicenter for all three groups was completely abolished and increased incrementally with distance from the epicenter. After AC105 treatment, however, smaller areas of spared gray and white matter were present 4 mm away from the epicenter up to 7.2 mm in the rostral direction from the epicenter.

Analysis of serum glial fibrillary acidic protein levels

Serum concentrations of GFAP over time in pigs treated with AC105, MgSO4, or saline are summarized in Figure 7. Pre-SCI, serum GFAP levels were not significantly different between the three groups (saline, MgSO4, and AC105) by two-way analysis of variance (ANOVA). The treatment intervention (saline, AC105, and $MgSO_4$) began at 4 h post-injury, and between 4 and 24 h, GFAP levels measured in AC105 and MgSO4 groups were significantly different than the saline group ($p < 0.001$) based on one-way repeated-measures ANOVA with Dunnet's post-test (Fig. 7). Forty-eight-hour data were not used for this analysis because of the limited number of measurements for which analyte levels were observed to be above the method's limit of quantitation. Regardless of dosing group, serum GFAP levels were observed to increase post-injury and then return to close to undetectable levels by 48 h.

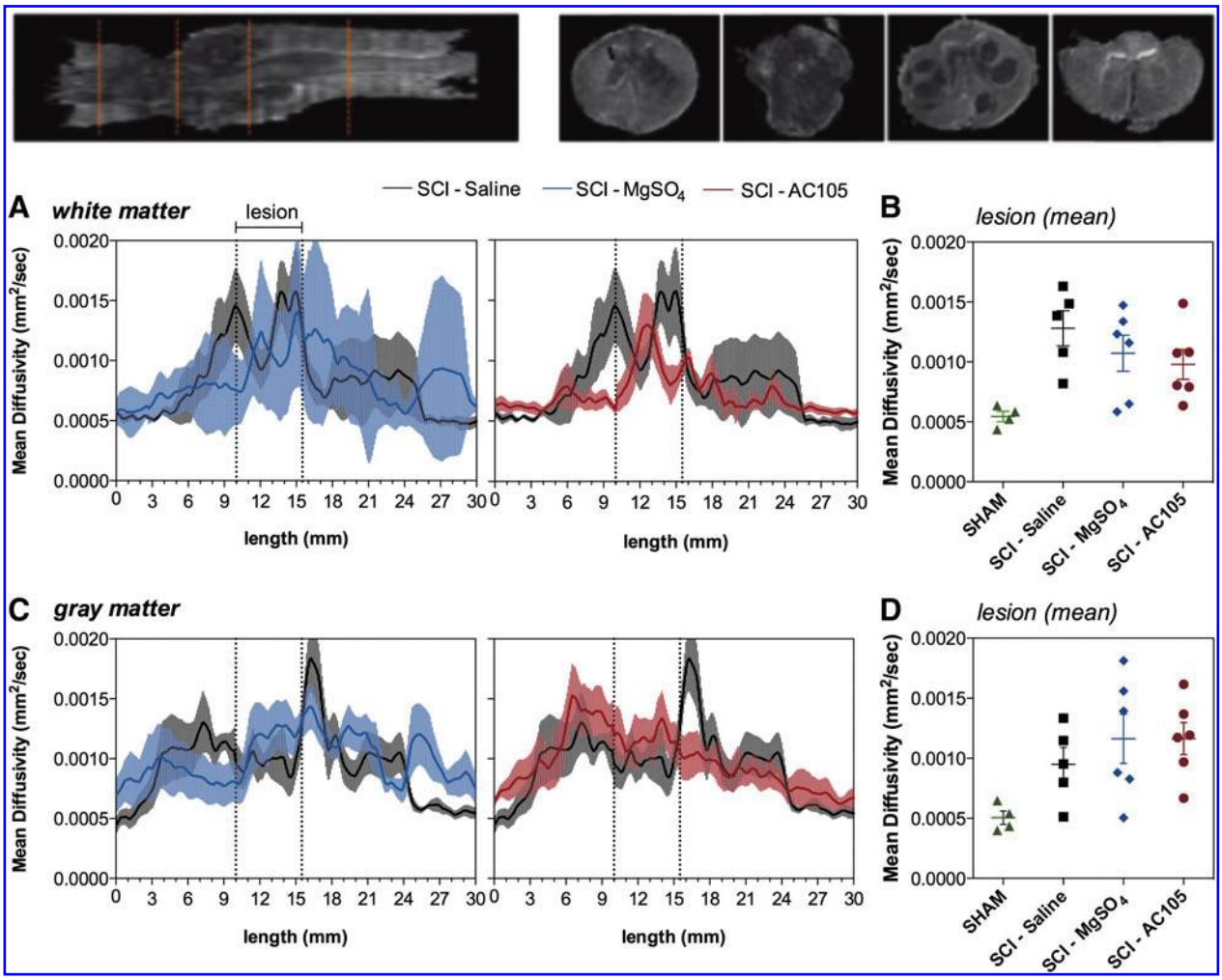

FIG. 3. Mean diffusivity in the spinal cord of SCI pigs treated with either saline, $MgSO_4$, or AC105. Top panel: images of mean diffusivity (MD) for spinal cord of SCI pigs. Orange dashed lines indicate the positions corresponding to the cross-sectional images on the right side of the figure. (**A**) White matter MD taken from longitudinal images of the spinal cord. The dashed line depicts the boundaries of the lesion core where the MD rostral and caudal from the epicenter were significantly different from MD at the epicenter. (**B**) Calculated mean white matter MD at the lesion core. (**C**) Gray matter MD taken from longitudinal images of spinal cord. (**D**) Calculated mean gray matter MD at the lesion core. All data are expressed as the mean ± standard error of the mean. Dots represent individual values of animals. Post-SCI, MD in the white and gray matter of the cord is increased rostral and caudal the site of injury (also observed in conditions of reduced membrane density such as during tissue degeneration). No statistical differences between the three treatment groups (saline, $MgSO_4$, and AC105) were observed. $MgSO_4$, magnesium sulphate; SCI, spinal cord injury. Color image is available online at www.liebertpub.com/neu

Analysis of cerebrospinal fluid magnesium levels

CSF Mg^{2+} levels were determined by OES-ICP in samples obtained pre-injury and from 0.5 to 30 h post-injury. A summary of CSF Mg^{2+} levels for the three groups is shown in Figure 8. CSF Mg^{2+} levels varied between ~0.7 and 1.0 mM across all times and treatment groups. Saline-treated animals experienced a modest decrease in CSF Mg^{2+} as compared to baseline. CSF Mg^{2+} levels appeared to be modestly higher than baseline in AC105- or $MgSO_4$-treated animals by 15–24 h post-injury, and this was maintained through the course of administration. There was no significant difference between CSF Mg^{2+} levels achieved between the AC105 and $MgSO_4$ formulations.

Discussion

This study was undertaken to evaluate a potentially neuroprotective pharmacologic agent, AC105, a proprietary formulation of $MgCl_2$ in PEG, in a porcine model of SCI. Magnesium has a long history of investigation as a neuroprotective agent in stroke and brain injury, and the formulation of $MgCl_2$ in PEG had been shown by independent laboratories and in different rodent injury models (thoracic and cervical SCI) to be beneficial post-SCI.[9–13,19] With these promising data from rodent injury models, we conducted this study to evaluate the robustness of this therapeutic effect in a large animal model. The pig spinal cord is much more similar in caliber and length to the human spinal cord than the rodent cord, and it has a more comparable CSF-filled intrathecal space. In addition to measuring behavioral, imaging, and histological outcomes, we evaluated changes in concentration of magnesium in the perilesional CSF and the potentially utility of serum GFAP as a biomarker of treatment effect.

In summary, despite the promise that was observed in rodent SCI models, when tested in a more clinical contusion/compression thoracic SCI model in the Yucatan minipig, the $MgCl_2$ in PEG

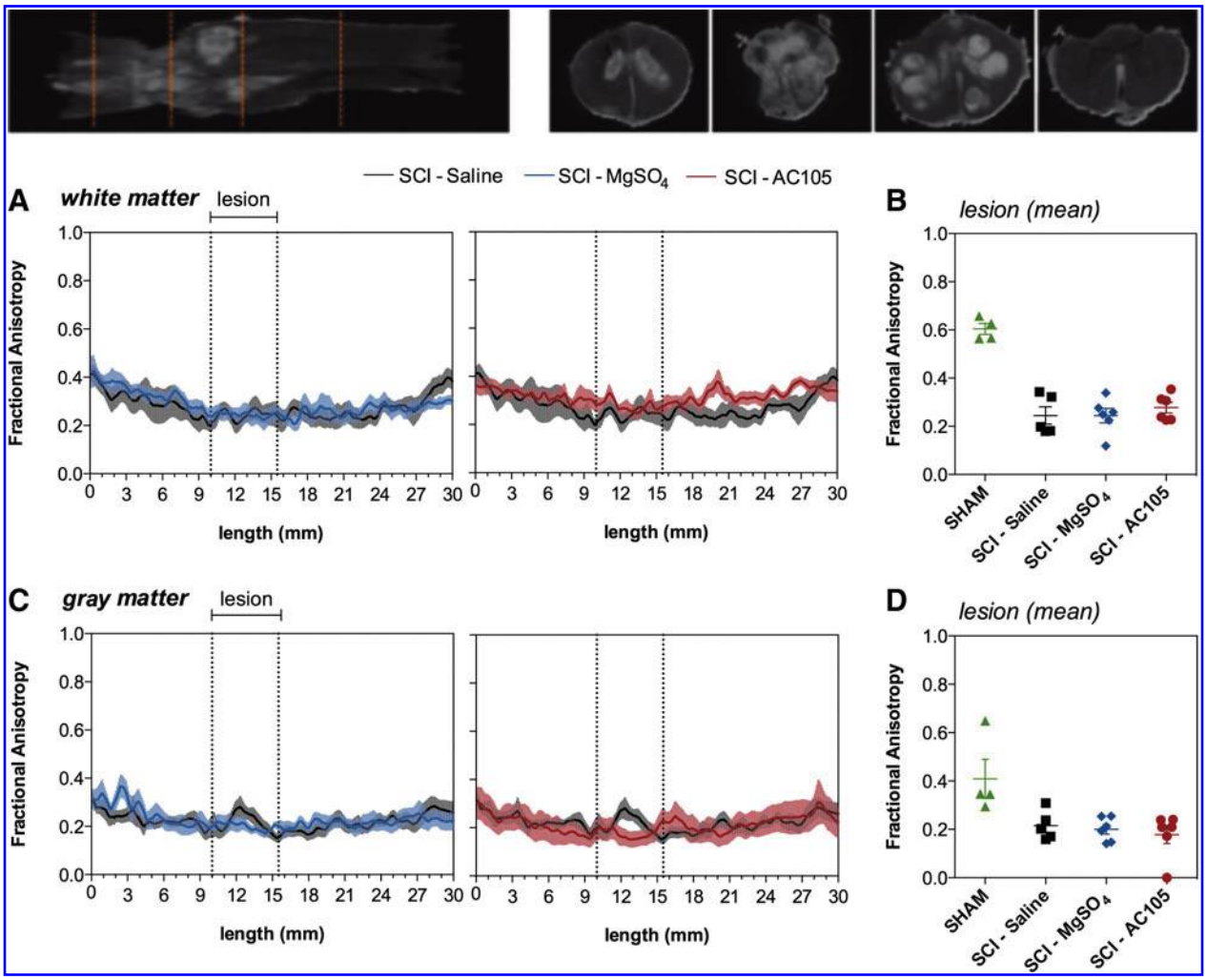

FIG. 4. Fractional anisotropy (FA) in spinal cord of SCI pigs treated with either saline, $MgSO_4$, or AC105. Top panel: images of FA for spinal cord of SCI pigs. Orange dashed lines indicate positions corresponding to the cross-sectional images on the right side of the figure. (**A**) White matter FA taken from longitudinal images of spinal cord. The dashed line depicts the boundaries of the lesion core where the FA rostral and caudal from the epicenter were significantly different from FA at the epicenter. (**B**) Calculated mean white matter FA at the lesion core. (**C**) Gray matter FA taken from longitudinal images of spinal cord. (**D**) Calculated mean gray matter FA at the lesion core. All data are expressed as the mean ± standard error of the mean. Dots represent individual values of animals. Post-SCI, FA decreases throughput the entire length of the cord analyzed (3 cm), consistent with diffuse disruption and disorganization through white and gray matter. No statistical differences between the three treatment groups (saline, $MgSO_4$, and AC105) are observed. $MgSO_4$, magnesium sulphate; SCI, spinal cord injury. Color image is available online at www.liebertpub.com/neu

formulation (AC105) did not alter behavioral, functional, imaging, or histological outcomes. With a 4-h treatment delay post-injury, the 30-min i.v. administration of AC105 every 6 h for 5 infusions in total did not improve behavioral recovery on our PTIBS locomotor scale, nor did it significantly alter hindlimb function as measured with 2D kinematic analysis. Interestingly, there was an apparent decrease in serum GFAP with both $MgSO_4$ and AC105 treatment, suggesting that there was some biological effect being mediated by the magnesium. Quantification of magnesium within CSF revealed that the AC105 formulation did not result in significantly higher levels of Mg within CSF than with the use of standard $MgSO_4$.

Although the efficacy observed in rodent models of SCI was not observed in this porcine SCI model, the nature of the injury model and its severity are important differences between these experimental paradigms. First, the severity of injury induced by our 20-cm weight-drop contusion with an additional 5 min of compression is very high, as is evidenced by the near complete obliteration of white and gray matter at the injury epicenter, with rostrocaudal extension of tissue loss over many millimeters (Figs. 5 and 6). This is considerably more severe than the resultant tissue loss observed in the axial plane and rostrocaudally with our previous rodent cervical and thoracic SCI studies in which we tested the magnesium-PEG treatment.[18,19] As seen in Figure 1, the resultant locomotor deficits in pigs with this injury severity are significant, with the recovery of only modest reciprocal hindlimb movement but no weight-bearing steps. In fact, the locomotor recovery on the PTIBS is generally limited to the animal transiently being able to lift its rump off the ground, and the treadmill kinematic analysis revealed very limited walking ability even with partial body-weight support. Possibly, the severity of tissue destruction also mitigated any potential benefit that the PEG might have in facilitating the distribution of Mg to the injury site, which was then reflected in

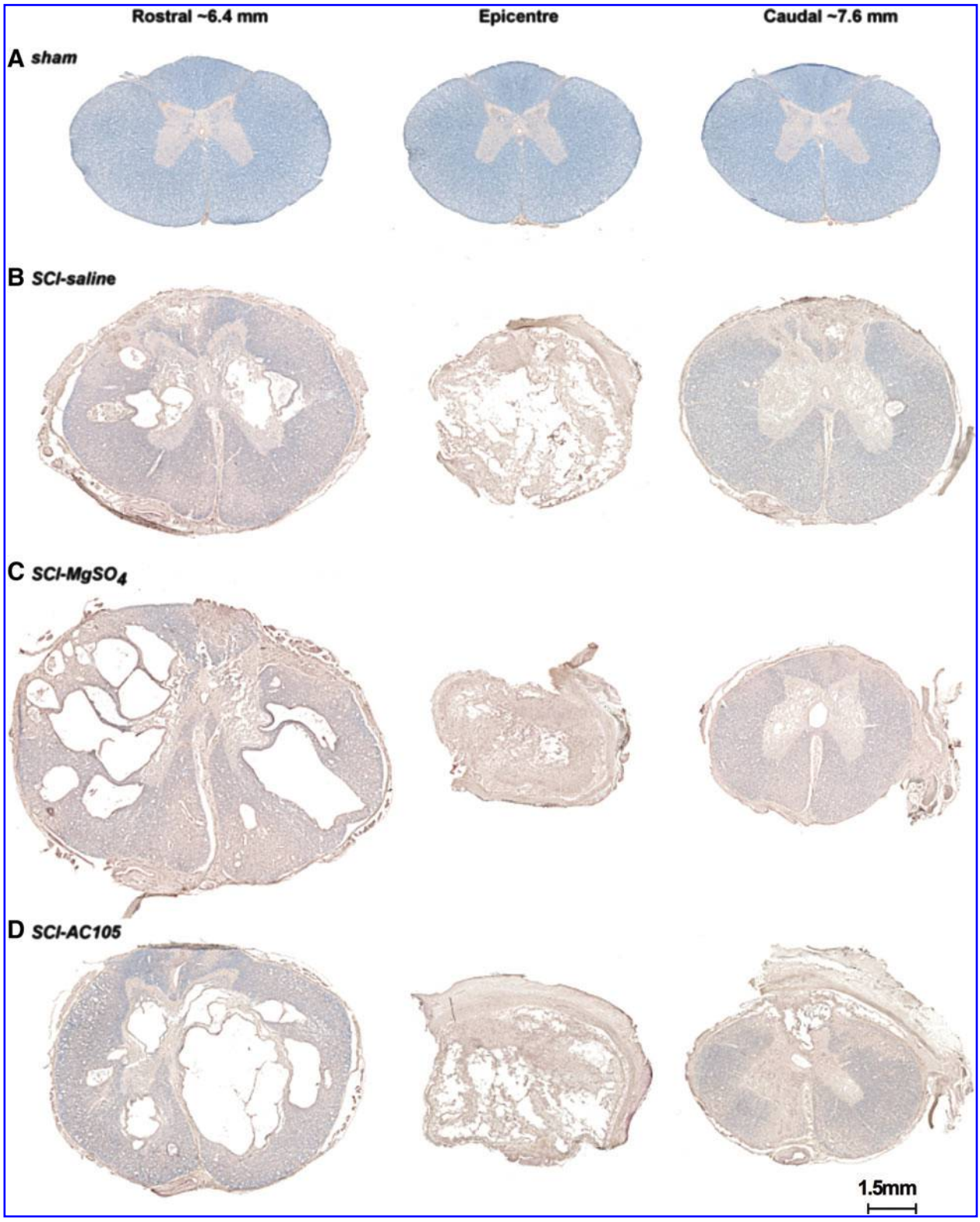

FIG. 5. Representative Eriochrome cyanine R–stained images of axially sectioned spinal cords. Cross-sectional sections of spinal cord tissue, at 12 weeks post-injury, stained with Eriochrome cyanine R to detect tightly packed myelin in (**A**) SHAM and spinal-cord–injured pigs treated with (**B**) saline, (**C**) $MgSO_4$, or (**D**) AC105. Scale bar = 1.5 cm. SCI results in large cavitations and tissue disorganization extending away from the lesion epicenter. $MgSO_4$, magnesium sulphate; SCI, spinal cord injury. Color image is available online at www.liebertpub.com/neu

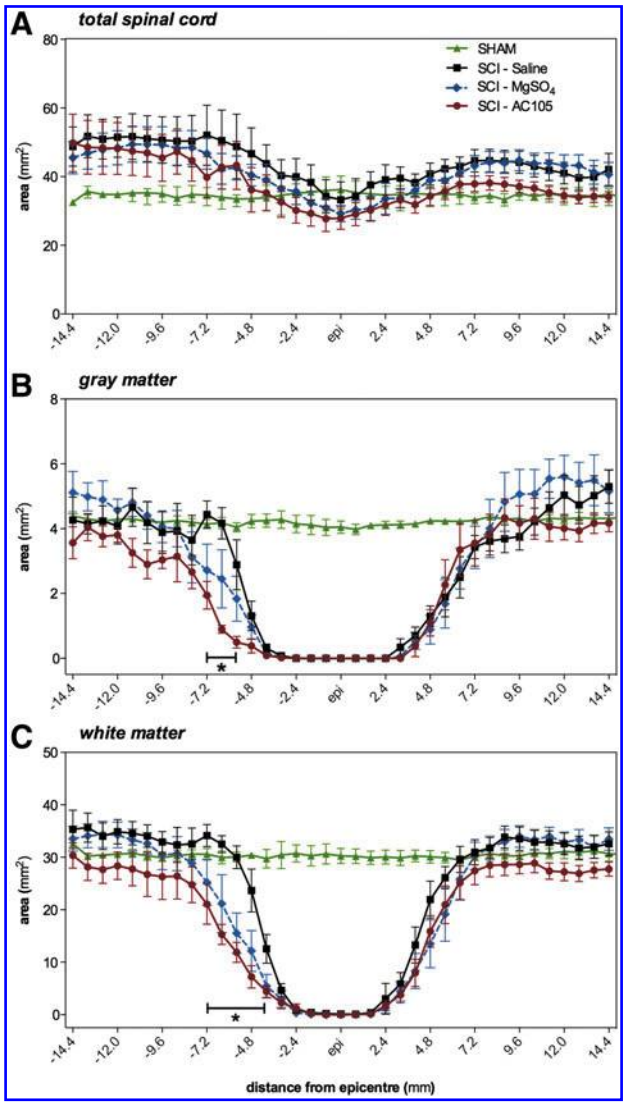

FIG. 6. Comparison of total spinal cord and spared tissue area between treatment groups (saline, $MgSO_4$, and AC105). (**A**) Total spinal cord area (**B**), spared gray matter, and (**C**) spared white matter determined by area measurements taken from axial sections of spinal cord tissue 800 μm apart in SHAM and spinal-cord–injured pigs treated with saline ($n=5$), $MgSO_4$ ($n=6$), or AC105 ($n=6$). Values are means ± standard error of the mean. Caudal to the epicenter (''epi''), the amount of spared gray and white matter is reduced in AC105 treatment. *AC105 significant difference compared to SCI-saline group: $p<0.05$. $MgSO_4$, magnesium sulphate; SCI, spinal cord injury. Color image is available online at www.liebertpub.com/neu

equivalent CSF magnesium levels in the Mg-PEG and $MgSO_4$ animals.

In any event, the results of this study highlight the potential for differential therapeutic efficacy when evaluating a potential therapeutic in a higher-order animal species (pig vs. rat) and with an ostensibly higher injury severity. Such a differential response was also observed in the rodent replication study of glibenclimide performed by Popovich and colleagues, in which the neuroprotective effects were observed only in the less-severe injuries.[34] This issue of differential therapeutic responses to varying injury severities and in higher-order animal species is important from a translational perspective. It emphasizes the concept that the therapeutic efficacy of an intervention be at least evaluated in models of different injury severities, particularly severe injuries that more closely resemble the severe motor-sensory complete or motor complete SCI in human patients. Based upon the high velocities with which the human spine column mechanically fails in simulated trauma[35–37] and the prolonged time (many hours) that the spinal cord often remains compressed, it is possible that even our pig model of SCI with its 20-cm weight drop and 5 min of compression (causing severe destruction at the injury site) insufficiently represents the severity of human spinal cord injuries that are typically enrolled into clinical trials of therapeutic interventions. If the efficacy of the Mg-PEG treatment could not be replicated in our pig model because of the severity of this injury, then it would stand to reason that it would be difficult to demonstrate its efficacy in a human clinical trial setting, which would invariably include severe (AIS A and B) types of paralysis.

In the current study, *ex vivo* DTI at 9.4T revealed an SCI-induced increase in MD and a decrease in FA at the injury site, similar as observed in animal models of SCI[38,39] and in patients with chronic complete and incomplete SCI.[40] DTI studies of the human spinal cord showed that especially FA values are correlated with motor score in patients with chronic cervical cord injury and in patients with nonhemorrhagic contusions.[40–44] In the current study, however, there was no difference between groups in terms of MD and FA values. This lack of a gross neuroprotective effect with AC105 was corroborated by histological analysis and quantification of white and gray matter sparing on axial sections through the injury site, although we found that quantification of these parameters on MR images tended to overestimate the extent of sparing (Supplementary Fig. 1) (see online supplementary material at http://www.liebertpub.com).

Evaluating locomotor performance is important for assessing the degree and quality of recovery post-SCI. The 10-point PTIBS assesses various aspects of hindlimb locomotion, such as flexion and extension movements, weight bearing, and stepping capacity. Using this 10-point scoring scale, we observed that independent of whether AC105 was administered, the majority of animals were only capable of executing occasional weight bearing hindlimb extensions that lifted the rump off the ground (i.e., PTIBS score 3 or 4), which is comparable to our previously published reports following a 20-cm weight drop.[18,45] The next point of improvement on the PTIBS (a score of 5) is assigned only when the animal is capable of some weight-supported stepping (>2 steps). It is possible that the absence of a significant improvement on the PTIBS with AC105 treatment was partially attributed to a ''ceiling'' effect in PTIBS scoring, with an improvement from a PTIBS score of 4–5 (representing the attainment of weight-supported stepping) being too large of an incremental improvement to achieve.

The number of animals assigned per group ($n=6$) was based on power analysis of PTIBS data collected from a previous study performed in our lab.[18] We performed a post-experiment power analysis to determine the sample size needed to detect a significant difference between the groups, given the variability that we actually observed. The power analysis indicated that, assuming equal group sizes and variability, a sample size of 16 for each group would be needed to distinguish a 1-point difference on the PTIBS (power of 80%, α set at 0.05). This dropped to sample sizes of 5 animals per group for detecting a more extreme 2-point PTIBS difference. We acknowledge that the higher variability in our current groups reduced the statistical power to detect potentially smaller functional changes that might be attributable to the AC105 treatment. Having said that, we also did not see a corresponding

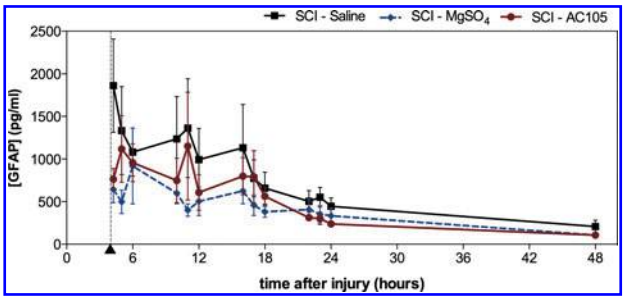

FIG. 7. Glial fibrillary acidic protein (GFAP) levels post-injury, pre-infusion, and post-infusion. Data are presented as mean ± standard error of the mean for each group over time. The treatment intervention (saline, AC105, and $MgSO_4$) began at 4 hours post-injury (▲). GFAP serum levels determined for AC105 and $MgSO_4$ groups are significantly lower between 4 and 24 h ($p < 0.001$), compared to the saline group, based on one-way repeated-measures analysis of variance with Dunnet's post-test. Forty-eight-hour data not used in analysis because of the limited number of measurements for which analyte levels were observed to be above the method's limit of quantitation. $MgSO_4$, magnesium sulphate; SCI, spinal cord injury. Color image is available online at www.liebertpub.com/neu

improvement in histological outcomes to suggest that we were simply underpowered to observe a behavioral improvement with AC105 treatment.

In the current study, we also collected detailed hindlimb kinematics during treadmill locomotion to identify changes in various gait parameters after AC105 treatment. No obvious differences between treatment groups were observed. A key issue in using the weight-support treadmill training is the frequency at which steps can be elicited. Obviously, regular spontaneous stepping can be challenging to obtain if animals are too severely impaired; however, even when there is some hindlimb control (PTIBS score 4), we observed that animals were predominantly dragging the dorsal

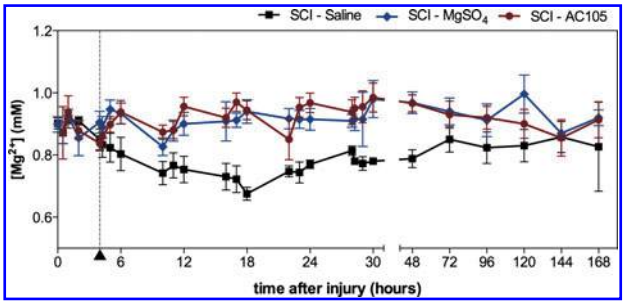

FIG. 8. Cerebrospinal fluid (CSF) magnesium levels from spinal-cord–injured animals treated with either saline, AC105, or $MgSO_4$. CSF magnesium (Mg^{2+}) levels were determined by OES-ICP in samples obtained pre-injury and from 0.5 to 170 h post-injury. Data are presented as mean ± standard error of the mean for each group over time from $n = 6$ animals per group. The treatment intervention (saline, AC105, and $MgSO_4$) began at 4 h post-injury (▲). Baseline CSF Mg^{2+} levels varied between ~0.7 and 1.0 mM across all three treatment groups. In the saline-treated animals, Mg^{2+} levels in CSF are immediately reduced post-SCI and remain low for up to 15–24 h post-injury. Notably, Mg^{2+} levels in the two magnesium-treated groups (AC105 and $MgSO_4$) showed no real sign of reduction from normal levels. $MgSO_4$, magnesium sulphate; OES-ICP, optical emission spectroscopy with inductively-coupled plasma excitation; SCI, spinal cord injury. Color image is available online at www.liebertpub.com/neu

surface of their hindlimbs on the treadmill. Our kinematics analysis would likely have been more interpretable if there had been an increase in stepping frequency, simply because more steps would be able to be included in the kinematic analysis of the hindlimbs.

In essence, this study, which utilized a porcine model of SCI, failed to replicate the promising therapeutic effects observed in rodent models of SCI. The use of large animal models such as the pig as an intermediary testing ground for the translation of novel therapeutics is a topic of interest for the SCI community, and the subject of a recent focus group discussion that we recently led.[46] We took the approach of wanting to know whether the promising therapeutic effects from rodent models of SCI could be translated to a large animal model. The results of our focus group initiative, which included representation from academia, industry, and funding agencies, revealed fairly divided opinions about the need for demonstrating efficacy of pharmacologic agents in large animal models before human translation. Notwithstanding this divided opinion, there was strong support for the notion that demonstrating improved behavioral outcomes in a large animal model would be considered as strong evidence for the robustness of therapeutic effect and would increase the perceived chances of the pharmacological agent working in humans.

In this regard, though testing in a large animal such as the pig may not be a translational ''requirement,'' there is certainly an understandable desire to evaluate the robustness of a therapy before committing to human trials. Interestingly, approximately half of the participants in our focus group initiative were of the opinion that the failure of a drug to effect any behavioral or nonbehavioral improvements in a large animal model was reason to stop it from moving toward human translation. Of course, we would acknowledge (as we did in our focus group initiative) that it has yet to be established what elements of pre-clinical efficacy testing in rodent, large animal, or primate models predict success or failure in human trials of SCI. It is, however, widely perceived that a therapy that can be shown to be effective in the hands of different investigators using different injury models and animal species would have a more likely chance of succeeding in clinical trials. The decision to test such a therapy in a large animal model is therefore complicated and depends on the balance of many considerations, such as the extent of rodent testing already performed, the extent to which a large animal model result would inform the decision to proceed with human studies, and the resources available to conduct such an initiative.

In addition to the question of efficacy, the use of a large animal model such as the pig may be helpful in addressing biodistribution and potential biomarkers of injury or outcome. Here, we utilized the more human-like CSF compartment of the pig to test levels of magnesium after the AC105 and standard $MgSO_4$ treatment. With a mean of 0.8 mM, the baseline CSF Mg^{2+} concentration in our pigs was similar to that reported in the CSF of humans and clinical patients.[17,47–50] The initial AC105 bolus marginally elevated CSF Mg^{2+} levels (12%), and after prolonged i.v. AC105 administration, CSF concentrations remained higher than during saline treatment. We were somewhat surprised to find that the AC105 formulation did not increase the magnesium levels within the CSF beyond that which was achieved with $MgSO_4$. In previous rodent studies, we had observed that the AC105 formulation resulted in much higher CSF concentrations of Mg than the standard $MgSO_4$ infusion (unpublished). It was this concept of enhanced Mg accumulation within the injured CNS that provided a strong rationale for the clinical applicability of the AC105 formulation, given the fact that the typical doses of $MgSO_4$ that had been utilized in rodent SCI

studies was much higher than what could be tolerated in humans. This suggests to us that biodistribution studies that utilize the CSF of rodents may not reflect what occurs in a larger animal model with a considerably larger intrathecal space containing significantly more CSF. Interestingly, we have internally conducted microdialysis studies to evaluate the intraparenchymal extracellular Mg levels that result from AC105 administration versus $MgSO_4$ administration in the rodent spinal cord and have found significantly higher levels of Mg in the dialysate of the AC105-treated animals (manuscript in preparation).

This study was conducted alongside the efforts to initiate a clinical trial of AC105 in acute human SCI (the Magnify study; ClinicalTrials.gov: NCT01750684). This prospective, randomized, placebo-controlled, phase 2a clinical trial was initiated across multiple institutions across North America in 2013 and enrolled the first cohort of 8 patients who received the first AC105 or placebo infusion within 12 h of injury. The trial then moved to a shortened time window of 9 h post-injury for the next cohort, but over 6 months of recruitment at seven trauma centers was only able to enroll 5 additional patients in the study. Because it was clear that the feasibility of recruiting within 9 h of injury was low, and the goal was ultimately to recruit patients within 6 h of injury, the decision was made to discontinue the study.

The decision to end the AC105 clinical trial was made after the results of this large animal study were known, although the lack of efficacy in this porcine SCI study was not the primary reason for ending the clinical trial. Of course, it does raise the intriguing question of whether it would be still prudent to continue with a lengthy, expensive clinical trial (if feasible) in the presence of reasonably strong pre-clinical rodent SCI efficacy data but with the absence of efficacy in a large animal study. Our large animal focus group initiative revealed that many in the field would not be in favor of moving forward with human translation in such a setting, although there was considerable disparity of opinion on this point. Both ends of the spectrum on this point are worth acknowledging. It is indeed true that we do not know what aspects of the behavioral recovery in a pig SCI model would predict success or failure of a treatment in human clinical trials. And so, one could rationally argue that if there is a reasonably strong and supportive body of preclinical evidence in rodent models of SCI, then a failed large animal study should not necessarily stop a treatment from moving forward to human investigation. On the other hand, if a therapy has a beneficial effect that is so hard to demonstrate in a large animal model despite the rigorously controlled conditions under which such an experiment is conducted, then it would be hard to be overly optimistic about its chances of revealing efficacy in the messy, heterogeneous setting of traumatic human SCI. In the end, the decision to aggressively pursue a shortened time window for patient recruitment (9 h and then eventually 6 h post-injury) revealed that the clinical trial was not feasible, and it was for this reason that the trial was stopped.

In conclusion, we did not observe a neuroprotective effect with administration of AC105 in this large animal model of SCI, given what we and others had demonstrated in rodent models. The long history of research on the use of magnesium in stroke, TBI, and SCI would indicate that magnesium is indeed conferring some degree of neuroprotection in these acute conductions. Translating this to an effective human application, however, is obviously challenging and will require further investigation that goes beyond proof of principle studies, but rather establishes a treatment paradigm with clinically relevant magnesium doses delivered within realistic time windows.

Acknowledgments

The authors thank the veterinary medical team and technicians at the UBC Center for Comparative Medicine (Vancouver, British Columbia, Canada) for their expertise in caring for the animals involved in these experiments. BKK holds the Canada Research Chair in Spinal Cord Injury.

Author Disclosure Statement

Brian K. Kwon is a paid member of the Scientific Advisory Board for Acorda Therapeutics. Jennifer F. Iaci, Donald C. Button, Andrea M. Vecchione, Andrey Konovalov, Patrick D. Sarmiere, Chi Ung, and Anthony O. Caggiano are all paid full-time employees of Acorda Therapeutics. For all other authors, no competing financial interests exist.

References

1. Lemke, M., Demediuk, P., McIntosh, T.K., Vink, R., and Faden, A.I. (1987). Alterations in tissue Mg++, Na+ and spinal cord edema following impact trauma in rats. Biochem. Biophys. Res. Commun. 147, 1170–1175.
2. Vink, R., McIntosh, T.K., Demediuk, P., and Faden, A.I. (1987). Decrease in total and free magnesium concentration following traumatic brain injury in rats. Biochem. Biophys. Res. Commun. 149, 594–599.
3. Heath, D.L., and Vink, R. (1999). Brain free magnesium concentration is predictive of motor outcome following traumatic axonal brain injury in rats. Magnes. Res. 12, 269–277.
4. Heath, D.L., and Vink, R. (1999). Concentration of brain free magnesium following severe brain injury correlates with neurologic motor outcome. J. Clin. Neurosci. 6, 505–509.
5. Lemke, M., Yum, S.W., and Faden, A.I. (1990). Lipid alterations correlate with tissue magnesium decrease following impact trauma in rabbit spinal cord. Mol. Chem. Neuropathol. 12, 147–165.
6. Mendez, D.R., Corbett, R., Macias, C., and Laptook, A. (2005). Total and ionized plasma magnesium concentrations in children after traumatic brain injury. Pediatr. Res. 57, 347–352.
7. Faden, A.I., Demediuk, P., Panter, S.S., and Vink, R. (1989). The role of excitatory amino acids and NMDA receptors in traumatic brain injury. Science 244, 798–800.
8. Mayer, M.L., Westbrook, G.L., and Guthrie, P.B. (1984). Voltage-dependent block by Mg^{2+} of NMDA responses in spinal cord neurones. Nature 309, 261–263.
9. Wiseman, D.B., Dailey, A.T., Lundin, D., Zhou, J., Lipson, A., Falicov, A., and Shaffrey, C.I. (2009). Magnesium efficacy in a rat spinal cord injury model. J. Neurosurg. Spine 10, 308–314.
10. Gok, B., Okutan, O., Beskonakli, E., and Kilinc, K. (2007). Effects of magnesium sulphate following spinal cord injury in rats. Chin. J. Physiol. 50, 93–97.
11. Ditor, D.S., John, S.M., Roy, J., Marx, J.C., Kittmer, C., and Weaver, L.C. (2007). Effects of polyethylene glycol and magnesium sulfate administration on clinically relevant neurological outcomes after spinal cord injury in the rat. J. Neurosci. Res. 85, 1458–1467.
12. Kaptanoglu, E., Beskonakli, E., Solaroglu, I., Kilinc, A., and Taskin, Y. (2003). Magnesium sulfate treatment in experimental spinal cord injury: emphasis on vascular changes and early clinical results. Neurosurg. Rev. 26, 283–287.
13. Kaptanoglu, E., Beskonakli, E., Okutan, O., Selcuk Surucu, H., and Taskin, Y. (2003). Effect of magnesium sulphate in experimental spinal cord injury: evaluation with ultrastructural findings and early clinical results. J. Clin. Neurosci. 10, 329–334.
14. Leeman, L. and Fontaine, P. (2008). Hypertensive disorders of pregnancy. Am. Fam. Physician. 78, 93–100.
15. Gowda, R.M. and Khan, I.A. (2004). Magnesium in treatment of acute myocardial infarction. Int. J. Cardiol. 96, 467–469.
16. Temkin, N.R., Anderson, G.D., Winn, H.R., Ellenbogen, R.G., Britz, G.W., Schuster, J., Lucas, T., Newell, D.W., Mansfield, P.N., Machamer, J.E., Barber, J., and Dikmen, S.S. (2007). Magnesium sulfate for neuroprotection after traumatic brain injury: a randomised controlled trial. Lancet. Neurol. 6, 29–38.

17. McKee, J.A., Brewer, R.P., Macy, G.E., Borel, C.O., Reynolds, J.D., and Warner, D.S. (2005). Magnesium neuroprotection is limited in humans with acute brain injury. Neurocrit. Care 2, 342–351.
18. Lee, J.H.T., Roy, J., Sohn, H.M., Cheong, M., Liu, J., Stammers, A.T., Tetzlaff, W., and Kwon, B.K. (2010). Magnesium in a polyethylene glycol formulation provides neuroprotection after unilateral cervical spinal cord injury. Spine (Phila. Pa. 1976) 35, 2041–2048.
19. Kwon, B.K., Roy, J., Lee, J.H.T., Okon, E., Zhang, H., Marx, J.C., and Kindy, M.S. (2009). Magnesium chloride in a polyethylene glycol formulation as a neuroprotective therapy for acute spinal cord injury: preclinical refinement and optimization. J. Neurotrauma 26, 1379–1393.
20. Saver, J.L., Starkman, S., Eckstein, M., Stratton, S., Pratt, F., Hamilton, S., Conwit, R., Liebeskind, D.S., Sung, G., and Sanossian, N.; FAST-MAG Investigators and Coordinators. (2014). Methodology of the Field Administration of Stroke Therapy–Magnesium (FAST-MAG) phase 3 trial: part 1—rationale and general methods. Int. J. Stroke 9, 215–219.
21. Saver, J.L., Starkman, S., Eckstein, M., Stratton, S., Pratt, F., Hamilton, S., Conwit, R., Liebeskind, D.S., Sung, G., and Sanossian, N.; FAST-MAG Investigators and Coordinators. (2014). Methodology of the Field Administration of Stroke Therapy–Magnesium (FAST-MAG) phase 3 trial: part 2—prehospital study methods. Int. J. Stroke 9, 220–225.
22. Aslanyan, S., Weir, C.J., Muir, K.W., and Lees, K.R.; IMAGES Study Investigators. (2007). Magnesium for treatment of acute lacunar stroke syndromes: further analysis of the IMAGES trial. Stroke 38, 1269–1273.
23. Saver, J.L., Kidwell, C., Eckstein, M., and Starkman, S.; FAST-MAG Pilot Trial Investigators. (2004). Prehospital neuroprotective therapy for acute stroke: results of the Field Administration of Stroke Therapy–Magnesium (FAST-MAG) pilot trial. Stroke 35, e106–e108.
24. Muir, K.W., Lees, K.R., Ford, I., and Davis, S.; Intravenous Magnesium Efficacy in Stroke (IMAGES) Study Investigators. (2004). Magnesium for acute stroke (Intravenous Magnesium Efficacy in Stroke trial): randomised controlled trial. Lancet 363, 439–445.
25. Gorelick, P.B., and Ruland, S. (2004). IMAGES and FAST-MAG: magnesium for acute ischaemic stroke. Lancet Neurol. 3, 330.
26. Lee, J.H.T., Jones, C.F., Okon, E.B., Anderson, L., Tigchelaar, S., Kooner, P., Godbey, T., Chua, B., Gray, G., Hildebrandt, R., Cripton, P., Tetzlaff, W., and Kwon, B.K. (2013). A novel porcine model of traumatic thoracic spinal cord injury. J. Neurotrauma 30, 142–159.
27. Klassen, L.M., and Menon, R.S. (2004). Robust automated shimming technique using arbitrary mapping acquisition parameters (RASTA-MAP). Magn. Reson. Med. 51, 881–887.
28. Behrens, T.E.J., Johansen-Berg, H., Woolrich, M.W., Smith, S.M., Wheeler-Kingshott, C.A.M., Boulby, P.A., Barker, G.J., Sillery, E.L., Sheehan, K., Ciccarelli, O., Thompson, A.J., Brady, J.M., and Matthews, P.M. (2003). Non-invasive mapping of connections between human thalamus and cortex using diffusion imaging. Nat. Neurosci. 6, 750–757.
29. Behrens, T.E.J., Woolrich, M.W., Jenkinson, M., Johansen-Berg, H., Nunes, R.G., Clare, S., Matthews, P.M., Brady, J.M., and Smith, S.M. (2003). Characterization and propagation of uncertainty in diffusion-weighted MR imaging. Magn. Reson. Med. 50, 1077–1088.
30. Smith, S.M., Jenkinson, M., Johansen-Berg, H., Rueckert, D., Nichols, T.E., Mackay, C.E., Watkins, K.E., Ciccarelli, O., Cader, M.Z., Matthews, P.M., and Behrens, T.E.J. (2006). Tract-based spatial statistics: voxelwise analysis of multi-subject diffusion data. Neuroimage 31, 1487–1505.
31. Smith, S.M., Jenkinson, M., Woolrich, M.W., Beckmann, C.F., Behrens, T.E.J., Johansen-Berg, H., Bannister, P.R., De Luca, M., Drobnjak, I., Flitney, D.E., Niazy, R.K., Saunders, J., Vickers, J., Zhang, Y., De Stefano, N., Brady, J.M., and Matthews, P.M. (2004). Advances in functional and structural MR image analysis and implementation as FSL. Neuroimage 23, Suppl. 1, S208–S219.
32. Woolrich, M.W., Jbabdi, S., Patenaude, B., Chappell, M., Makni, S., Behrens, T., Beckmann, C., Jenkinson, M., and Smith, S.M. (2009). Bayesian analysis of neuroimaging data in FSL. Neuroimage 45, 1 Suppl., S173–S186.
33. Rabchevsky, A.G., Fugaccia, I., Sullivan, P.G., and Scheff, S.W. (2001). Cyclosporin A treatment following spinal cord injury to the rat: behavioral effects and stereological assessment of tissue sparing. J. Neurotrauma 18, 513–522.
34. Popovich, P.G., Lemeshow, S., Gensel, J.C., and Tovar, C.A. (2012). Independent evaluation of the effects of glibenclamide on reducing progressive hemorrhagic necrosis after cervical spinal cord injury. Exp. Neurol. 233, 615–622.
35. Ivancic, P.C., Pearson, A.M., Tominaga, Y., Simpson, A.K., Yue, J.J., and Panjabi, M.M. (2007). Mechanism of cervical spinal cord injury during bilateral facet dislocation. Spine (Phila. Pa. 1976) 32, 2467–2473.
36. Wilcox, R.K., Boerger, T.O., Hall, R.M., Barton, D.C., Limb, D., and Dickson, R.A. (2002). Measurement of canal occlusion during the thoracolumbar burst fracture process. J. Biomech. 35, 381–384.
37. Panjabi, M.M., Kifune, M., Wen, L., Arand, M., Oxland, T.R., Lin, R.M., Yoon, W.S., and Vasavada, A. (1995). Dynamic canal encroachment during thoracolumbar burst fractures. J. Spinal Disord. 8, 39–48.
38. Nevo, U., Hauben, E., Yoles, E., Agranov, E., Akselrod, S., Schwartz, M., and Neeman, M. (2001). Diffusion anisotropy MRI for quantitative assessment of recovery in injured rat spinal cord. Magn. Reson. Med. 45, 1–9.
39. Deo, A.A., Grill, R.J., Hasan, K.M., and Narayana, P.A. (2006). In vivo serial diffusion tensor imaging of experimental spinal cord injury. J. Neurosci. Res. 83, 801–810.
40. Ellingson, B.M., Kurpad, S.N., and Schmit, B.D. (2008). Ex vivo diffusion tensor imaging and quantitative tractography of the rat spinal cord during long-term recovery from moderate spinal contusion. J. Magn. Reson. Imaging 28, 1068–1079.
41. Chang, Y., Jung, T.-D., Yoo, D.S., and Hyun, J.K. (2010). Diffusion tensor imaging and fiber tractography of patients with cervical spinal cord injury. J. Neurotrauma 27, 2033–2040.
42. Cheran, S., Shanmuganathan, K., Zhuo, J., Mirvis, S.E., Aarabi, B., Alexander, M.T., and Gullapalli, R.P. (2011). Correlation of MR diffusion tensor imaging parameters with ASIA motor scores in hemorrhagic and nonhemorrhagic acute spinal cord injury. J. Neurotrauma 28, 1881–1892.
43. Koskinen, E.A., Hakulinen, U., Brander, A.E., Luoto, T.M., Ylinen, A., and Ohman, J.E. (2014). Clinical correlates of cerebral diffusion tensor imaging findings in chronic traumatic spinal cord injury. Spinal Cord 52, 202–208.
44. Koskinen, E., Brander, A., Hakulinen, U., Luoto, T., Helminen, M., Ylinen, A., and Ohman, J. (2013). Assessing the state of chronic spinal cord injury using diffusion tensor imaging. J. Neurotrauma 30, 1587–1595.
45. Streijger, F., Lee, J.H.T., Chak, J., Dressler, D., Manouchehri, N., Okon, E.B., Anderson, L.M., Melnyk, A.D., Cripton, P.A., and Kwon, B.K. (2015). The effect of whole-body resonance vibration in a porcine model of spinal cord injury. J. Neurotrauma 32, 908–921.
46. Kwon, B.K., Streijger, F., Hill, C.E., Anderson, A.J., Bacon, M., Beattie, M.S., Blesch, A., Bradbury, E.J., Brown, A., Bresnahan, J.C., Case, C.C., Colburn, R.W., David, S., Fawcett, J.W., Ferguson, A.R., Fischer, I., Floyd, C.L., Gensel, J.C., Houle, J.D., Jakeman, L.B., Jeffery, N.D., Jones, L.A., Kleitman, N., Kocsis, J., Lu, P., Magnuson, D.S., Marsala, M., Moore, S.W., Mothe, A.J., Oudega, M., Plant, G.W., Rabchevsky, A.S., Schwab, J.M., Silver, J., Steward, O., Xu, X.M., Guest, J.D., and Tetzlaff, W. (2015). Large animal and primate models of spinal cord injury for the testing of novel therapies. Exp. Neurol. 269, 154–168.
47. Brewer, R.P., Parra, A., Borel, C.O., Hopkins, M.B., and Reynolds, J.D. (2001). Intravenous magnesium sulfate does not increase ventricular CSF ionized magnesium concentration of patients with intracranial hypertension. Clin. Neuropharmacol. 24, 341–345.
48. Ko, S.H., Lim, H.R., Kim, D.C., Han, Y.J., Choe, H., and Song, H.S. (2001). Magnesium sulfate does not reduce postoperative analgesic requirements. Anesthesiology 95, 640–646.
49. Heipertz, R., Eickhoff, K., and Karstens, K.H. (1979). Magnesium and inorganic phosphate content in CSF related to blood-brain barrier function in neurological disease. J. Neurol. Sci. 40, 87–95.
50. Thurnau, G.R., Kemp, D.B., and Jarvis, A. (1987). Cerebrospinal fluid levels of magnesium in patients with preeclampsia after treatment with intravenous magnesium sulfate: a preliminary report. Am. J. Obstet. Gynecol. 157, 1435–1438.

Address correspondence to:
Brian K. Kwon, MD, PhD, FRCSC
Department of Orthopedics
University of British Columbia
6th Floor
Blusson Spinal Cord Center
VGH
818 West 10th Avenue
Vancouver, British Columbia
Canada V5Z 1M9

E-mail: brian.kwon@ubc.ca

This article has been cited by:

1. Kim Kyoung-Tae, Streijger Femke, So Kitty, Manouchehri Neda, Shortt Katelyn, Okon Elena Borisovna, Tigchelaar Seth, Fong Allan, Morrison Charlotte, Keung Martin, Sun Jenny, Liu Ella, Cripton Peter Alexander, Kwon Brian K.. Differences in Morphometric Measures of the Uninjured Porcine Spinal Cord and Dural Sac Predict Histological and Behavioral Outcomes after Traumatic Spinal Cord Injury. *Journal of Neurotrauma*, ahead of print. [Abstract] [Full Text] [PDF] [PDF Plus] [Supplementary Material]
2. He Zhao, Qing-Ling Sun, Li-Jun Duan, Yong-Dong Yang, Yu-Shan Gao, Ding-Yan Zhao, Yang Xiong, He-Jun Wang, Jia-Wei Song, Kai-Tan Yang, Xiu-Mei Wang, Xing Yu. 2019. Is cell transplantation a reliable therapeutic strategy for spinal cord injury in clinical practice? A systematic review and meta-analysis from 22 clinical controlled trials. *European Spine Journal* **28**:5, 1092-1112. [Crossref]
3. Carolina Rouanet, Gisele Sampaio Silva. Update on Traumatic Spinal Cord Injury 253-260. [Crossref]
4. Jayne Donovan, Steven Kirshblum. 2018. Clinical Trials in Traumatic Spinal Cord Injury. *Neurotherapeutics* **15**:3, 654-668. [Crossref]
5. Streijger Femke, So Kitty, Manouchehri Neda, Tigchelaar Seth, Lee Jae H.T., Okon Elena B., Shortt Katelyn, Kim So-Eun, McInnes Kurt, Cripton Peter, Kwon Brian K.. 2017. Changes in Pressure, Hemodynamics, and Metabolism within the Spinal Cord during the First 7 Days after Injury Using a Porcine Model. *Journal of Neurotrauma* **34**:24, 3336-3350. [Abstract] [Full Text] [PDF] [PDF Plus] [Supplementary Material]
6. A Wang-Leandro, M K Hobert, N Alisauskaite, P Dziallas, K Rohn, V M Stein, A Tipold. 2017. Spontaneous acute and chronic spinal cord injuries in paraplegic dogs: a comparative study of in vivo diffusion tensor imaging. *Spinal Cord* **55**:12, 1108-1116. [Crossref]
7. Jared T. Wilcox, Kajana Satkunendrarajah, Yasmin Nasirzadeh, Alex M. Laliberte, Alyssa Lip, David W. Cadotte, Warren D. Foltz, Michael G. Fehlings. 2017. Generating level-dependent models of cervical and thoracic spinal cord injury: Exploring the interplay of neuroanatomy, physiology, and function. *Neurobiology of Disease* **105**, 194-212. [Crossref]
8. Huang Zhihong, Filipovic Zoran, Mp Nandakumar, Ung Chia, Troy Erika L., Colburn Raymond W., Iaci Jennifer F., Hackett Craig, Button Donald C., Caggiano Anthony O., Parry Tom J.. 2017. AC105 Increases Extracellular Magnesium Delivery and Reduces Excitotoxic Glutamate Exposure within Injured Spinal Cords in Rats. *Journal of Neurotrauma* **34**:3, 685-694. [Abstract] [Full Text] [PDF] [PDF Plus]
9. Liam M. Koehn, Natassya M. Noor, Qing Dong, Sing-Yan Er, Lachlan D. Rash, Glenn F. King, Katarzyna M. Dziegielewska, Norman R. Saunders, Mark D. Habgood. 2016. Selective inhibition of ASIC1a confers functional and morphological neuroprotection following traumatic spinal cord injury. *F1000Research* **5**, 1822. [Crossref]
10. Liam M. Koehn, Qing Dong, Sing-Yan Er, Lachlan D. Rash, Glenn F. King, Katarzyna M. Dziegielewska, Norman R. Saunders, Mark D. Habgood. 2016. Selective inhibition of ASIC1a confers functional and morphological neuroprotection following traumatic spinal cord injury. *F1000Research* **5**, 1822. [Crossref]